Rat Liver Aromatic L-Amino Acid Decarboxylase: Spectroscopic and Kinetic Analysis of the Coenzyme and Reaction Intermediates†

Hideyuki Hayashi, Hiroyuki Mizuguchi, and Hiroyuki Kagamiyama*

Department of Biochemistry, Osaka Medical College, Takatsuki, Osaka 569, Japan

Received September 8, 1992; Revised Manuscript Received October 29, 1992

ABSTRACT: The physicochemical properties of the coenzyme in rat liver aromatic L-amino acid decarboxylase (AADC) expressed in *Escherichia coli* have been studied by spectroscopic analysis of the enzyme, its reaction intermediates, and its complexes with substrate analogs. The enzyme, having one pyridoxal 5′-phosphate (PLP) per subunit, shows a prominent absorption maximum at 335 nm and a weaker one at 425 nm. The spectrum did not essentially change in the pH range of 6.0–8.0. When the coenzyme was excited at 335 nm, it emitted fluorescence primarily at 520 nm. The structure for the absorption at 335 nm was ascribed to the enolimine form of the PLP–lysine Schiff base. On the reaction of AADC with L-3,4-dihydroxyphenylalanine (L-dopa), the absorption of PLP showed biphasic changes before reaching a steady-state. Results of both pre-steady-state and steady-state kinetic analyses were consistent with the model that the reaction proceeds as shown in the equation: $E + S \rightleftarrows X_1 \rightleftarrows X_2 \rightarrow E + P$. The rate constant was determined for each step, and the K_m value for L-dopa was obtained as 0.086 mM. The absorption spectra of the two intermediates, X_1 and X_2, were postulated from the calculation of the absorption changes during the first and the second steps of the reaction in which X_1 and X_2 showed an absorption maximum at 425 and 380 nm, respectively, with a concomitant decrease in absorbance at 335 nm. These predicted absorption spectra of X_1 and X_2 showed striking resemblances to those of AADC complexed with dihydroxyphenylacetic acid (DOPAc) and L-dopa methyl ester (DopaOMe), respectively. These compounds are substrate analogs for the adsorption complex and the "external aldimine" structure, respectively. The results suggest that X_1 and X_2 conform to these structures. AADC and the AADC–DOPAc complex showed a positive CD at wavelength bands corresponding to the absorption spectra, but the AADC–DopaOMe complex showed a very weak CD over 300 nm. We now conclude that the 335-nm-absorbing species is an internal Schiff base placed in an apolar environment and the species is involved in the catalytic reaction by interacting with substrate amino acids.

Aromatic L-amino acid decarboxylase (aromatic L-amino acid carboxy-lyase, EC 4.1.1.28) (AADC)[1] catalyzes the irreversible decarboxylation reaction of several aromatic L-amino acids, including dopa, *m*-tyrosine, *p*-tyrosine, phenylalanine, 5-hydroxytryptophan, and tryptophan. AADC contains pyridoxal phosphate (PLP) as a coenzyme and shows absorption maxima at 335 and 425 nm, besides the protein absorption at 280 nm (Ando-Yamamoto et al., 1987; Dominici et al., 1987; Voltattorni et al., 1979; Nakazawa et al., 1974). One of the characteristic properties of this enzyme is its prominent absorption maximum at 335 nm, which is twice as large as that at 425 nm. Most PLP-dependent enzymes have absorption bands in the range of 400–440 nm, and it is generally agreed that the absorption peak in this region represents an internal Schiff base (ketoenamine form, see structure III in Scheme I) of PLP with the active-site lysine residue. However, the absorption at around 330–350 nm in PLP enzymes represents a variety of structures, such as an enolimine tautomer of a PLP–lysine Schiff base (e.g., II in Scheme I) (Shaltiel & Cortijo, 1970; Johnson et al., 1970), a substituted aldamine structure (e.g., I in Scheme I) (Misono & Soda, 1977), and an unprotonated PLP–lysine Schiff base (Minelli et al., 1979). In order to study the mechanism of action of AADC, it is important to clarify the structure which absorbs at around 335 nm. For this purpose, detailed spectrophotometric studies on the enzyme itself as well as on the reaction of the enzyme with substrate(s) and substrate analogs are required. In this study, we observed the absorption, fluorescence, and CD spectra of AADC and its complexes with substrate analogs. Also, we have analyzed the reaction of AADC with L-dopa using a stopped-flow spectrophotometer. On the basis of these spectrophotometric data, we discuss the structure of the coenzyme and its involvement in catalysis.

MATERIALS AND METHODS

Chemicals. L-3,4-Dihydroxyphenylalanine (L-dopa) was obtained from Nacalai Tesque (Kyoto, Japan). L-Dopa methyl ester was from Sigma. Dihydroxyphenylacetic acid was from Aldrich and was crystallized twice from hot benzene before use. Phenylhydrazine hydrochloride was from Kishida Chemicals (Osaka, Japan) and was crystallized twice from hot ethanol. Restriction enzymes were from Takara Shuzo (Kyoto, Japan). All other chemicals were the highest grade commercially available.

Enzyme Preparation. Rat liver AADC was expressed in *E. coli* as follows. A plasmid pUC9 containing the *Eco*RI–*Eco*RV fragment of rat liver AADC cDNA (Tanaka et al., 1989) in its *Eco*RI–*Sma*I site was excised with *Acc*III and *Hin*dIII. The *Acc*III–*Hin*dIII fragment (the *Acc*III site was blunted with S1 nuclease) was ligated to the *Nco*I–*Hin*dIII

† This work was supported by Grant-in-Aid 04780211 from the Ministry of Education, Science, and Culture of Japan.

* Author to whom correspondence should be addressed.

[1] Abbreviations: AADC, aromatic L-amino acid decarboxylase; PLP, pyridoxal 5′-phosphate; DOPAc, dihydroxyphenylacetic acid; DopaOMe, L-dopa *O*-methyl ester; PIPES, piperazine-*N*,*N*′-bis(2-ethanesulfonic acid); MES, 2-(*N*-morpholino)ethanesulfonic acid; CAPS, 3-(cyclohexylamino)propanesulfonic acid; SDS, sodium dodecyl sulfate; CD, circular dichroism.

0006-2960/93/0432-812$04.00/0

Scheme I

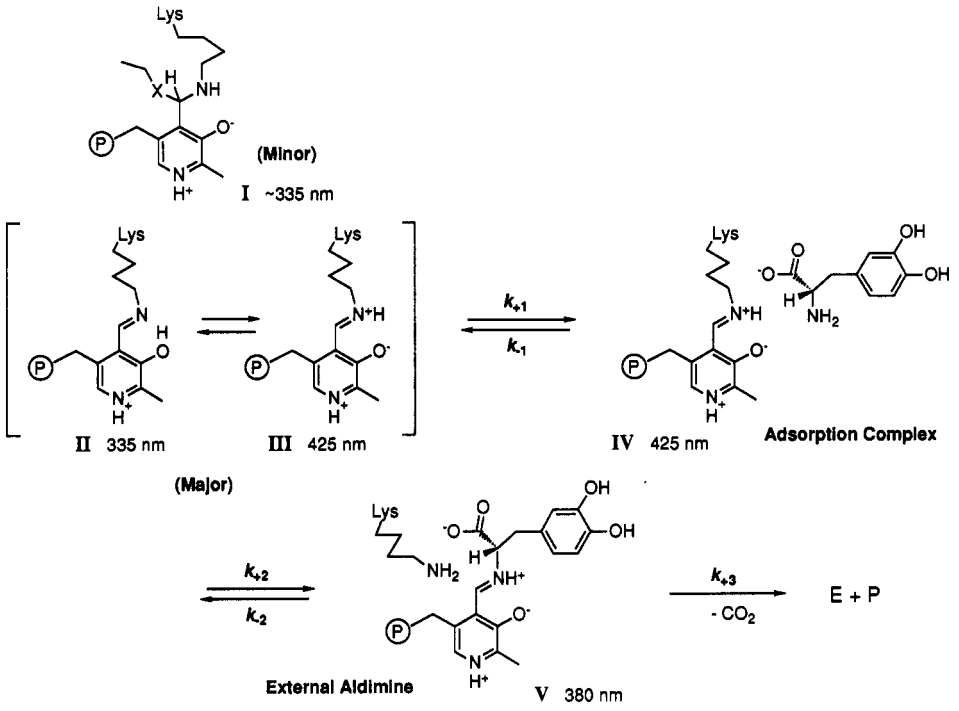

site of pKK233-2 (Pharmacia) using a synthetic linker:

5'>CATGGATTCTCGTGAATTTCGA
CTAAGAGCACTTAAAGCT<5'

This linker contains the sequence just downstream of the initiation codon and was designed to maximize the base-pairing with 16S rRNA of *E. coli* (Sprengart et al., 1990) without altering the amino acid sequence. The resultant plasmid, named pKKAADCII, was expressed in *E. coli* JM109 (*recA1*, *endA1*, *gyrA96*(Nal^r), *thi*, *hsdR17*($r_k^-m_k^+$), *supE44*, *relA1*, Δ(*lac-proAB*), F'[*traD36*, *proAB*$^+$, *lacI*^{q}, *lacZ*ΔM15]). The cells were grown in YT medium in the presence of 0.05 mg/mL ampicillin for 24 h at 37 °C. The enzyme was purified as described previously (Ando-Yamamoto et al., 1987) except that the heat treatment was omitted and DEAE-cellulose was replaced by DEAE-Toyopearl 650M. About 30 mg of purified AADC was usually obtained from 30 g of cells, or 10 L of culture medium. The purified enzyme showed mobility in SDS–polyacrylamide gel electrophoresis similar to that of the enzyme purified from rat liver. The N-terminal sequence, analyzed by the Applied Biosystems protein sequencer 470A, was Met-Asp-Ser-Arg-Glu-Phe-, which is the same as the N-terminal sequence of rat liver AADC deduced from its cDNA sequence (Tanaka et al., 1989).

Preparation of Apoenzyme. The coenzyme PLP was removed from AADC as a phenylhydrazone according to the method of Yonaha et al. (1975) with modifications. To the solution containing about 4 mg of holoenzyme in 0.9 mL of 0.5 M potassium phosphate buffer, pH 7.5, was added 0.1 mL of 50 mM phenylhydrazine hydrochloride which was neutralized with NaOH. The solution was kept at 37 °C for 30 min and then passed through Sephadex G-25 (15 × 52 mm) equilibrated with 0.5 M potassium phosphate buffer, pH 7.5.

Determination of Protein Concentration. The concentration of AADC in a solution was determined spectrophotometrically. The apparent molar extinction coefficients used were ϵ_M = 7.75 × 10^4 $M^{-1}\cdot cm^{-1}$ for the apoenzyme and ϵ_M = 7.90 × 10^4 $M^{-1}\cdot cm^{-1}$ for PLP form of the enzyme at 280 nm. These values were determined on the basis of the exact protein concentration in the solution determined by the amino acid analysis.

Spectrophotometric Measurements. Absorption and fluorescence spectra were measured using a Hitachi 557 spectrophotometer and 850 fluorescence spectrophotometer, respectively. CD spectroscopy was carried out on a Jasco J-600 spectropolarimeter. The buffer solution contained 50 mM PIPES–NaOH, pH 7.0, for absorption and CD measurements and 10 mM potassium phosphate buffer, pH 7.0, for fluorescence analysis. Protein concentrations were (1–2) × 10^{-5} M. For pH titration experiments, 50 mM Good's buffer component (MES, PIPES, or CAPS) was used to adjust the pH of the solution.

Stopped-flow spectrophotometry was performed by an Applied Photophysics stopped-flow SF.17MW spectrophotometer and Union Giken RA-401. The dead times for this system were 2.3 and 1.4 ms, respectively, under a pressure of 5.0 $kg\cdot cm^{-2}$.

Steady-State Analysis of the Decarboxylation of L-*Dopa by AADC.* The decarboxylation of L-dopa by AADC was performed in a 1-mL reaction mixture containing 50 mM PIPES–NaOH, pH 7.0, 5 μM PLP, and 1 pmol of AADC. The amount of product dopamine was measured fluorometrically as described earlier (Ando-Yamamoto et al., 1987). The rate of dopamine formation was determined for substrate concentrations between 0.01 and 1 mM.

RESULTS

Absorption Spectra of AADC and Its Complexes with Substrate Analogs. AADC has absorption maxima at 335 and 425 nm (Figure 1). The absorption at 335 nm is twice as large as that at 425 nm. The spectrum showed no change at pH values between 6.0 and 7.0 and showed only a slight increase in the absorbance at 335 nm and a decrease at 425 nm when the pH was raised from 7.0 to 8.0 (data not shown). This suggests that the two absorption bands (425- and 335-nm bands) do not represent different protonated forms. The spectra of AADC in the presence of substrate analogs,

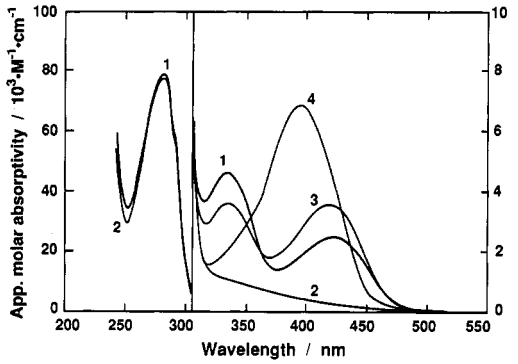

FIGURE 1: Spectra of AADC. Absorption spectra were taken in 50 mM PIPES–NaOH buffer, pH 7.0. Phenylhydrazine-treated AADC was prepared as described under Materials and Methods. The enzyme concentration was 10 μM. (1) AADC. (2) Phenylhydrazine-treated AADC. (3) AADC + 1.74 mM DOPAc. (4) AADC + 0.55 mM DopaOMe. The K_d values were 0.10 mM for DOPAc and 0.050 mM for DopaOMe.

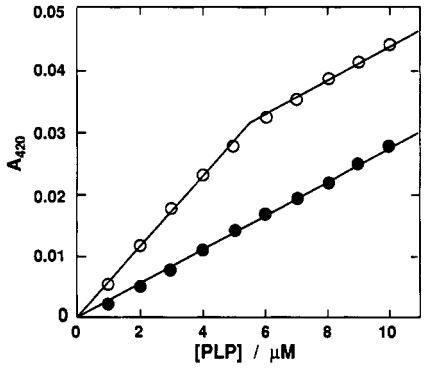

FIGURE 2: Titration of the phenylhydrazine-treated AADC with PLP. To 50 mM PIPES solution (pH 7.0) and 50 mM PIPES solution (pH 7.0) containing 5 μM phenylhydrazine-treated AADC was added PLP successively. Absorption spectra between 300 and 550 nm were taken after each addition of PLP, and the absorbance at 420 nm was plotted against the concentration of PLP. Open circles, 50 mM PIPES, pH 7.0, containing 5 μM AADC. Closed circles, 50 mM PIPES, pH 7.0.

dihydroxyphenylacetic acid (DOPAc) and L-dopa methyl ester (DopaOMe), were measured. The spectra of AADC with nearly fully bound analogs are shown in Figure 1. The binding of DOPAc to AADC increased the absorbance at 425 nm and decreased the 335-nm absorbance. On the other hand, binding of DopaOMe to AADC decreased the absorbance both at 335 nm and at 425 nm and increased the absorbance at 392 nm. These observed spectral changes showed a hyperbolic dependency on analog concentrations.

Preparation of Apo-AADC and Its Characterization. The phenylhydrazine-treated AADC essentially lost the two absorption peaks at 335 and 425 nm (Figure 1). However, substantial absorption remained between 500 and 300 nm, in which there was an increase toward shorter wavelength. The phenylhydrazine-treated AADC was titrated with PLP in order to evaluate the PLP binding ability of this apoenzyme (Figure 2). The titration curve of 5 μM apo-AADC with PLP showed a bend at a PLP concentration of 5.5 μM. This indicates that 1.1 mol of PLP is bound to 1 mol of AADC subunit.

Fluorescence Spectra. The fluorescence spectra of the holoenzyme and the phenylhydrazine-treated enzyme were measured (Figure 3). When the holoenzyme was excited at 425 nm, a fluorescence emission maximum was observed at 520 nm. The phenylhydrazine-treated AADC did not show fluorescence upon excitation at 425 nm. When the holoenzyme was excited at 335 nm, fluorescence emission maxima were

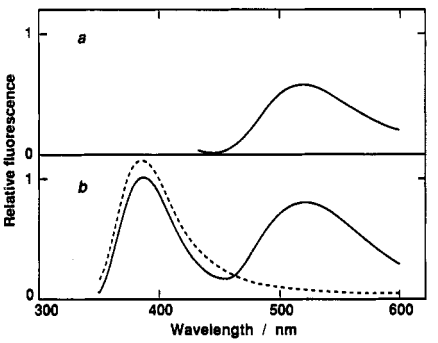

FIGURE 3: Fluorescence spectra of the native and phenylhydrazine-treated AADC. Fluorescence spectra were measured in 50 mM potassium phosphate buffer, pH 7.0. The enzyme concentration was 8×10^{-7} M. (a) Excitation at 425 nm. (b) Excitation at 335 nm. Solid line, native AADC. Dashed line, phenylhydrazine-treated AADC.

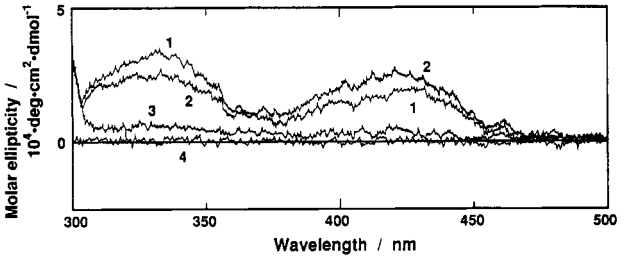

FIGURE 4: Circular dichroism spectra of AADC. CD spectra were measured in 50 mM PIPES–NaOH buffer, pH 7.0. The enzyme concentration was 10 μM. (1) AADC. (2) AADC + 1.74 mM DOPAc. (3) AADC + 0.55 mM DopaOMe. (4) Phenylhydrazine-treated AADC.

found at 387 nm and at 520 nm. When excited at 335 nm, the phenylhydrazine-treated AADC showed fluorescence at 387 nm similar to that of the holoenzyme but did not emit fluorescence at 520 nm. This indicates that the 520-nm fluorescence species arises from PLP moiety which is reversibly bound to the enzyme. When emission was observed at 520 nm, the excitation spectra exhibited maxima at 340 and 430 nm for the holoenzyme (data not shown). The fluorescence excitation spectrum was similar to the absorption spectrum in Figure 1.

CD Spectra. The CD spectra of the holoenzyme, the apoenzyme, and the holoenzyme complexed with DOPAc and DopaOMe were measured (Figure 4). The CD spectrum of AADC showed a positive Cotton effect at around both 335 nm and 425 nm; these wavelengths corresponded well to the wavelengths of the absorption peaks. Upon addition of DOPAc, the ellipticity at 335 nm decreased, whereas that at 425 nm increased. Thus, the CD spectra of the holoenzyme showed changes similar to those in the absorption spectra on binding of DOPAc. On the other hand, the ellipticity of AADC between 300 and 550 nm almost disappeared on addition of DopaOMe. Phenylhydrazine-treated AADC did not show a Cotton effect above 300 nm.

Time-Dependent Reaction of AADC with L-Dopa. The changes in the absorbance of AADC on reaction with L-dopa were studied in a stopped-flow spectrophotometer (Figure 5). Upon mixing the enzyme with 0.2 mM L-dopa, a rapid increase in the absorption at 420 nm occurred within 20 ms. The absorbance then decreased slowly within 0.5 s. In both the fast and slow phases, the absorbance changes proceeded exponentially, and the apparent rate constants (k_{app}'s) were obtained from these reaction curves. When the reaction was monitored at other wavelengths, the direction and amplitude of absorption changes differed from those in Figure 5, although

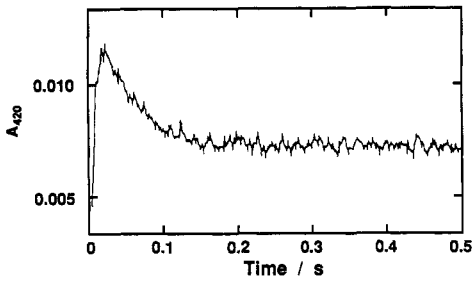

FIGURE 5: Time course of the reaction of AADC with L-dopa. AADC (5 μM) was mixed with 0.2 mM L-dopa in a stopped-flow spectrophotometer at 25 °C, pH 7.0 (50 mM PIPES–NaOH). The absorbance at 420 nm was monitored within 0.5 s.

the k_{app} values for the reactions were independent of the wavelength. At wavelengths above 406 nm, there was a rapid increase followed by a slow decrease in absorbance. At wavelengths below 406 nm and above 355 nm, there was a rapid increase followed by a slow increase in absorbance. At 406 nm, only a rapid increase in absorbance was observed.

The values of k_{app} for the fast and the slow phases were plotted against L-dopa concentrations (Figure 6). The value of k_{app} for the fast phase increased linearly with increasing substrate concentration, whereas that for the slow phase showed a nonlinear relationship with substrate concentration and indicated the saturation kinetics. The above observations could be analyzed most simply by assuming that the reaction of AADC with L-dopa proceeds in such a manner as is shown in eq 1 where E = enzyme, S = substrate, X_1 and X_2 =

$$E + S \underset{k_{-1}}{\overset{k_{+1}}{\rightleftarrows}} X_1 \underset{k_{-2}}{\overset{k_{+2}}{\rightleftarrows}} X_2 \overset{k_{+3}}{\rightarrow} E + P \qquad (1)$$

intermediates 1 and 2, respectively, P = product, k_{+1}, k_{+2}, and k_{+3} = rate constants for the forward reaction, and k_{-1} and k_{-2} = rate constants for the reverse reaction.

Solving the linear differential equations (1a and 2a) (see the Appendix) where the substrate concentration is sufficiently high, i.e., $[S] \gg (k_{-1} + k_{+2} + k_{-2} - k_{+3})/k_{+1}$, two apparent rate constants were obtained:

$$k_{app,fast} = k_{+1}[S] + k_{-1} \qquad (2)$$

$$k_{app,slow} = k_{+2} + k_{-2} + k_{+3} \qquad (3)$$

As shown in Figure 6, experimental data at high concentrations of the substrate were fitted well to the above equations, and the following values of rate constants were obtained: $k_{+1} = 5.1 \times 10^5$ $M^{-1}\cdot s^{-1}$, $k_{-1} = 70$ s^{-1}, and $k_{+2} + k_{-2} + k_{+3} = 27$ s^{-1}.

Estimation of the values of the kinetic parameters k_{+2}, k_{-2}, and k_{+3} was attempted as follows. As shown in Figure 5, the absorbance reached a constant value, which reflected the fact that the reaction of AADC with L-dopa reached a steady-state. The difference in the absorbance between the steady-state and the initial state was estimated by extrapolating the exponential curve of the fast phase to $t = 0$, and the estimated ΔA values were plotted against the substrate concentrations (Figure 7). We have chosen the wavelength 406 nm, at which no absorbance change occurs during the "slow" phase. This means that the intermediates X_1 and X_2 have the same absorbance at 406 nm (see Figure 8). Therefore, the absorbance of AADC at steady-state can be determined by monitoring only the "fast" phase. The plots in Figure 7 fitted well to a hyperbolic curve. This reflected the dependence of $[X_1]_{ss}$ and $[X_2]_{ss}$ (the concentrations of X_1 and X_2 at steady-state, respectively) on substrate concentrations (see eq 11a and 12a in the Appendix). Therefore, by fitting the data to eq 12a, the K_m value was determined to be 0.086 mM. By substituting the known values for k_{+1}, k_{-1}, and $k_{+2} + k_{-2} + k_{+3}$, eq 13a was transformed to $k_{-2} + k_{+3} + k_{+2}k_{+3}/70$ $s^{-1} = 16.9$ s^{-1}. From steady-state analysis of the decarboxylation of L-dopa by AADC, the value of $k_{cat} \equiv k_{+2}k_{+3}/(k_{+2} + k_{-2} + k_{+3})$ had been obtained as 5.0 s^{-1}. Therefore, $k_{+2}k_{+3} = 135$ s^{-2}. From these relationships, the values of k_{+2}, k_{+3}, and k_{-2} were calculated to be 12.0, 11.2, and 3.8 s^{-1}, respectively.

Absorption Spectra of the Intermediates. Because all of the kinetic parameters in eq 1 had been obtained, we could demonstrate the spectra of the intermediates X_1 and X_2 by calculation. AADC was mixed with a saturating concentration of L-dopa (1 mM) so that the concentration of the free enzyme could be negligible after the first phase of the reaction. The spectrum of X_1 was deduced by simply adding the amplitude of the absorption changes at a given wavelength (every 10-nm intervals) in the first phase of the reaction to the spectrum of AADC (Figure 8). In order to evaluate the spectral nature of the intermediate X_2, we expressed the molar absorptivity of AADC under the "steady-state" condition:

$$\epsilon_{ss} = \frac{k_{-2} + k_{+3}}{k_{+2} + k_{-2} + k_{+3}}\epsilon_{X_1} + \frac{k_{+2}}{k_{+2} + k_{-2} + k_{+3}}\epsilon_{X_2} \qquad (4)$$

where ϵ_{X_1} and ϵ_{X_2} denote the extinction coefficients of the intermediates X_1 and X_2, respectively. Since ϵ_{ss}, ϵ_{X_1}, and the rate constants were known values, the value of ϵ_{X_2} was derived from eq 4. The spectrum of the intermediate X_2 thus obtained is shown in Figure 8. As shown in Figure 8, the intermediate X_1 exhibited absorption maxima at around 335 and 425 nm, whereas the intermediate X_2 exhibited its maximum at around 380 nm. The absorption spectra of X_1 and X_2 showed a striking similarity to those of AADC complexed with DOPAc and DopaOMe, respectively.

DISCUSSION

AADC shows absorption bands at 335 and 425 nm. The nature of the 335-nm-absorbing species of AADC is puzzling. In the case of pig kidney AADC, an unprotonated PLP–lysine aldimine (Schiff base) structure was suggested for the 335-nm-absorbing species and a protonated aldimine structure for the 425-nm-absorbing species (Minelli et al., 1979). However, the unprotonated aldimine structure usually absorbs at around 360 nm (Kallen et al., 1984). Moreover, the spectrum of rat liver AADC, which is very similar to that of pig kidney enzyme, showed little change with altering pH. These findings indicate that the 335-nm- and 425-nm-absorbing species of AADC do not represent different ionic forms. In some PLP-dependent enzymes, the nature of the 335-nm-absorbing species has been suggested to be either the enolimine tautomer placed in an apolar environment (Shaltiel & Cortijo, 1970; Johnson et al., 1970) or the aldamine complex of the Schiff base imine with an unidentified second nucleophile (Misono & Soda, 1977; O'Leary, 1971). We then examined whether or not the latter two structures can represent the 335-nm-absorbing species in AADC.

The two species, enolimine tautomer and substituted aldamine, can be distinguished by fluorescence spectroscopy (Shaltiel & Cortijo, 1970; Johnson et al., 1970; Vázquez et al., 1991). The enolimine tautomer (II in Scheme I) of protonated PLP–Lys aldimine should show fluorescence at around 500 nm, and the emission wavelength must be the same as that of the ketoenamine tautomer (III in Scheme I). When the fluorescence spectra of AADC were examined, the holoenzyme showed an emission band at 520 nm with excitation

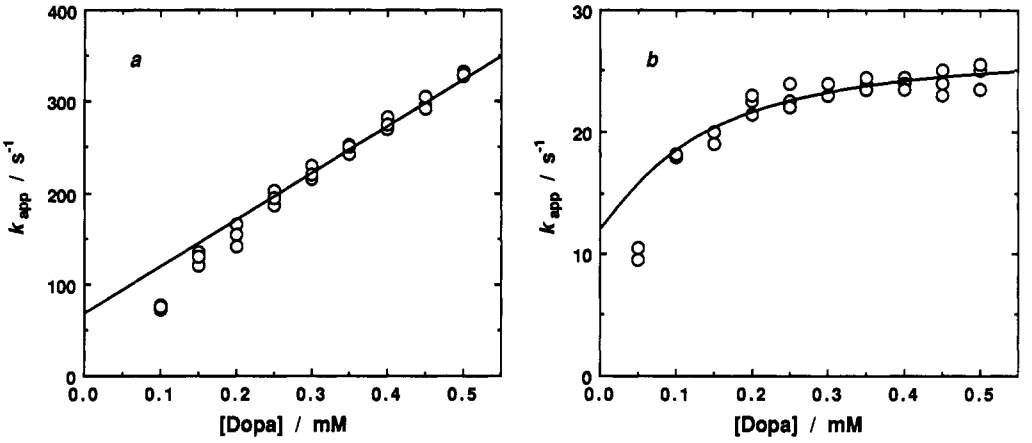

FIGURE 6: Plots of the apparent rate constants versus substrate concentrations. Apparent rate constants (k_{app}) of the "fast" and the "slow" reaction phases were obtained from the reaction curve in Figure 1 (see text for detail). At least three k_{app} values were obtained for each substrate concentration. Solid lines are theoretical drawings using eq 9a and 10a. (a) Fast phase. (b) Slow phase.

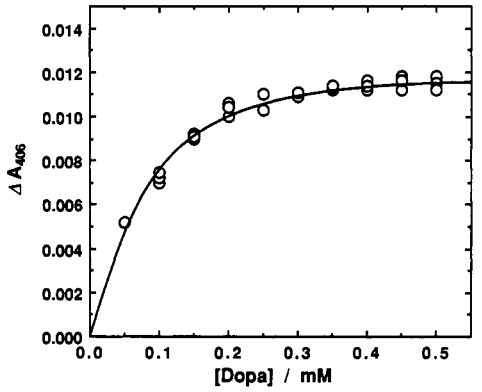

FIGURE 7: Dependency of the amplitude of absorbance changes during pre-steady-state reaction on substrate concentration. The conditions are the same as in Figure 2. At least three values of amplitude were obtained for each substrate concentration. The solid line is a theoretical drawing using the equation $\Delta A_{406} = \Delta A_{406,max}[S]/(K_m + [S])$ and K_m = 0.086 mM, which was derived from eq 12a.

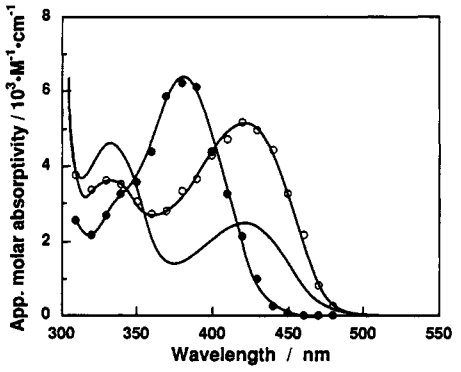

FIGURE 8: Absorption spectra of the intermediates of the reaction of AADC with L-dopa. The reaction of 5 μM AADC with 1 mM L-dopa was followed at every 10-nm wavelength. The reaction conditions are the same as in Figure 2. The absorbance changes from the free enzyme, E, to the intermediate, X_1, and from E to the intermediate X_2 were obtained (see text for detail). By adding these values to the absorption spectrum of the free enzyme, the spectra of the intermediates X_1 (○) and X_2 (●) were obtained.

at either 335 or 425 nm (Figure 3). The excitation spectrum between 300 and 500 nm was matched with the optical absorption spectrum. When AADC was treated with phenylhydrazine, most of the absorption at both the 335-nm and 425-nm bands disappeared. The resultant apoenzyme completely lacked fluorescence at 520 nm. All these observations agree with the consideration that most of the 335-nm absorption is attributed to the enolimine tautomer of protonated aldimine. In pig kidney AADC, fluorescence was not observed at around 500 nm upon excitation at 335 nm (Voltattorni et al., 1979), and an extremely low intensity of emission at 490 nm was observed upon excitation at 420 nm. It was suggested that the fluorescence at around 500 nm was strongly quenched by pig kidney AADC protein. Obviously, this quenching was not substantial in rat liver AADC. It is interesting to note that rat liver AADC and pig kidney AADC, which share a similar absorption spectrum (Ando-Yamamoto et al., 1987; Dominici et al., 1987; Voltattorni et al., 1979) and primary structure (Tanaka et al., 1989; Maras et al., 1991), have different fluorescence properties. Pig kidney AADC contains one PLP per dimer structure (Voltattorni et al., 1971, 1979), and rat liver AADC contains two PLP per dimeric enzyme protein (Dominici et al., 1987; this work); the relationship of the difference in coenzyme binding mode to the difference in fluorescence properties between the two enzymes needs further studies.

Some of the spectroscopic properties of PLP in rat liver AADC had been investigated (Dominici et al., 1987). It was observed that one molecule of PLP was released from one molecule of AADC subunit. This is consistent with our observation that AADC apoenzyme, prepared by phenylhydrazine treatment, binds one PLP per subunit. In their studies, however, hydroxylamine-treated AADC lost 425-nm absorption but had a peak at 335 nm similar to that present in the holoenzyme. It was then concluded that the absorbance at 335 nm is not due to the active coenzyme (Dominici et al., 1987). We showed that phenylhydrazine treatment greatly decreased the absorbance at 335 nm and most of the 335-nm absorption is due to the protonated PLP–Lys aldimine. Probably the bulky phenyl group of PLP–phenylhydrazone accelerated the resolution of the coenzyme from the enzyme active site and was the effective factor in removing PLP from AADC.

As shown in Figure 3b, AADC exhibited fluorescence at 387 nm upon excitation at 335 nm. Fluorescence at around 390 nm has not been observed for the enolimine tautomer upon excitation at around 330 nm (Shaltiel & Cortijo, 1970; Johnson et al., 1970). Therefore, the 387-nm fluorescent species is unlikely to be the enolimine tautomer. Since substituted aldamines and other phosphopyridoxyl derivatives show fluorescence at around 390 nm with excitation at 335 nm, it is likely that the 387-nm fluorescence species do not contain any double bonds conjugated with the pyridine ring. The same fluorescent species at 387 nm were observed when

the phenylhydrazine-treated enzyme was examined as shown in Figure 3b. This apoenzyme completely lacked fluorescence at 520 nm. This observation with phenylhydrazine-treated enzyme suggests that the 387-nm fluorescence is associated with some kind of chromophore that is attached to apoenzyme. This is supported by the fact that there are unremovable chromophores present in the apoenzyme which absorb between 500 and 300 nm (Figure 1). Despite repeated treatments with either phenylhydrazine, 0.1 M NaOH, or guanidine hydrochloride, such a chromophore could not be removed (data not shown). This unknown chromophore shows a fluorescence emission maximum at 387 nm and an excitation maximum at 335 nm. It may be related to the chromophore in the β-subform of aspartate aminotransferase (Metzler et al., 1987) or some sort of adduct of a Schiff base with a nucleophilic group proposed for lysine aminotransferase (Misono & Soda, 1977). Because the chromophore is stable toward denaturation, thiol and amino groups are unlikely candidates for such nucleophiles. We suggest that imidazole or indole can be such a nucleophilic group, since both of them form a stable C–C bond.

The kinetic analysis of the reaction of AADC with its most efficient substrate, L-dopa, demonstrated the presence of two intermediates, X_1 and X_2. X_1 appears to be formed by the intermolecular association of AADC and L-dopa, and X_2 appears to be formed from X_1 by an intramolecular rearrangement. The absorption spectra of X_1 and X_2 (Figure 8) were proposed as exhibiting a maximum at 425 and 380 nm, respectively. In pig kidney AADC, Minelli et al. (1979) observed that two intermediates were formed during the reaction of the enzyme with L-dopa. Although they did not obtain the spectra of these intermediates, they predicted that the 420-nm-absorbing species is formed first and then followed by formation of the second intermediate absorbing at 380–390 nm. Their prediction coincided with our results. The absorption spectra of X_1 and X_2 showed close similarity to those of the complex of AADC with DOPAc and DopaOMe, respectively (Figures 1 and 8). DOPAc does not form an external Schiff base with PLP since it lacks a primary amino group. DopaOMe contains an esterified carboxyl group and is not feasible to be decarboxylated. Therefore, the complexes of AADC with DOPAc and DopaOMe are considered to be the models for studying the adsorption complex of AADC with L-dopa and the "external" aldimine intermediate, respectively. It is, therefore, highly probable that the spectrum assigned to the intermediate X_1 represents the adsorption complex of AADC with L-dopa and that for X_2 represents the external aldimine. Because a substantial part of the absorption band at 335 nm of the free enzyme (E) vanished upon formation of the intermediates X_1 and X_2, the catalytic reaction of AADC with L-dopa seemed to correlate with the spectral change of the 335-nm band. Therefore, it is likely that the 335-nm-absorbing species participates in forming a Schiff base with L-dopa.

In pig kidney AADC, the binding of DOPAc caused an increase in absorption at 425 nm and a decrease at 335 nm, and the binding of DopaOMe caused the appearance of a new absorption at 390 nm (Barboni et al., 1982). However, in each case, a prominent absorption at 335 nm remained. The pig kidney AADC apoenzyme nearly lost the 430-nm band, but still exhibited a significant amount of absorption at 335 nm, which was similar in strength to that of the holoenzyme (Voltattorni et al., 1971). In rat liver AADC apoenzyme, both the 425-nm and 335-nm bands were essentially lost. In the pig kidney enzyme, hydroxylamine was used to remove PLP; therefore, the difference in spectra of these AADC apoenzymes could be due to resolution techniques used. However, as only one PLP molecule was detected per one molecule of dimeric enzyme, pig kidney AADC possibly contains one inactive chromophore in its dimer structure (Voltattorni et al., 1979), and this may be the cause of the remaining absorption of the pig kidney AADC–substrate analog complex at 335 nm.

The CD spectra of AADC in the presence of substrate analogs showed that the ellipticity assigned for the coenzyme ring is almost maintained for the AADC–DOPAc complex but is lost for the AADC–DopaOMe complex. These findings agree well with the mechanism that, in the adsorption complex, the structure and conformation of the Schiff base between PLP and Lys303 are almost conserved, and when PLP undergoes transaldimination to form a new Schiff base with substrates, there is a great change in the conformation of the coenzyme.

Scheme I summarizes the proposed intermediates in the reactions of AADC and L-dopa. Absorption maxima for these intermediates and kinetic parameters are also shown. The increase in absorbance at 425 nm upon binding of L-dopa or DOPAc with AADC is accompanied by the decrease in 335-nm absorbance. This phenomenon was explained by a shift in equilibrium between enolimine (II) and ketoenamine (III), in which this equilibrium favored ketoenamine formation. The binding of L-dopa or DOPAc to AADC, which would cause the increase in polarity of the local environment surrounding the coenzyme, may contribute to the shift in equilibrium. In the species IV, dopa is expressed with its carboxyl group dissociated and amino group nonprotonated. The latter is because the amino group must be deprotonated before it reacts with the internal aldimine. The K_m value for L-dopa increased as the pH decreased from 7.[2] The K_d value for DopaOMe increased from 0.012 to 0.21 mM as the pH decreased from 8.0 to 6.0. From these observations, we consider that L-dopa and DopaOMe bind to AADC with its amino group nonprotonated, or if the amino group is protonated, the proton on the amino group moves to an unidentified base that has a pK_a value around 6–8 in the active site. The K_d value for DOPAc slightly decreased from 0.11 to 0.092 mM as the pH decreased from 8.0 to 6.0. Therefore, DOPAc is supposed to bind to AADC with its carboxyl group dissociated. This suggests that L-dopa also binds to AADC as a carboxylate ion.

The intermediate X_2, assigned to the external aldimine (V in Scheme I), absorbs at 380 nm. This wavelength is somewhat blue-shifted compared to the value obtained from the ketoenamine Schiff base (IV in Scheme I). We speculate that the reason for this blue-shift is due to (1) the formation of new hydrogen bonds upon either PLP or the substrate, (2) the nonplanar structure of the external aldimine with its imine group perpendicular to the ring, or (3) the special environment of the active site. As the nonplanar form of external aldimine is not a suitable structure for decarboxylation, (2) seems to be less probable. The precise nature awaits further investigation.

ACKNOWLEDGMENT

We thank Drs. T. Tanaka and H. Wada, Faculty of Medicine, Osaka University, for donating the rat liver AADC cDNA. We are also grateful to Dr. K. Soda, Institute for Chemical Research, Kyoto University, for the use of the spectropolarimeter.

[2] Hayashi et al., unpublished results.

APPENDIX

From eq 1, two differential equations (1a and 2a) are obtained:

$$E + S \underset{k_{-1}}{\overset{k_{+1}}{\rightleftarrows}} X_1 \underset{k_{-2}}{\overset{k_{+2}}{\rightleftarrows}} X_2 \overset{k_{+3}}{\rightarrow} E + P \quad (1)$$

$$d[E]/dt = -k_{+1}[E][S] + k_{-1}[X_1] + k_{+3}[X_2] \quad (1a)$$

$$d[X_2]/dt = k_{+2}[X_1] - (k_{-2} + k_{+3})[X_2] \quad (2a)$$

At steady-state

$$k_{+3}[X_2]_{ss} = k_{+2}[X_1]_{ss} - k_{-2}[X_2]_{ss} = k_{+1}[E]_{ss}[S] - k_{-1}[X_1]_{ss} \quad (3a)$$

$$[E]_{tot} = [E] + [X_1] + [X_2] = [E]_{ss} + [X_1]_{ss} + [X_2]_{ss} \quad (4a)$$

where the subscript ss means the value at steady-state.

If the reaction is close to steady-state:

$$[E] = [E]_{ss} + \Delta[E]$$

$$[X_1] = [X_1]_{ss} + \Delta[X_1] \quad (5a)$$

$$[X_2] = [X_2]_{ss} + \Delta[X_2]$$

Using eq 3a–5a, the differential equations (1a and 2a) are rearranged to

$$-\frac{d\Delta[E]}{dt} = (k_{+1}[S] + k_{-1})\Delta[E] + (k_{-1} - k_{+3})\Delta[X_2] \quad (6a)$$

$$-\frac{d\Delta[X_2]}{dt} = k_{+2}\Delta[E] + (k_{+2} + k_{-2} + k_{+3})\Delta[X_2] \quad (7a)$$

The apparent rate constants are obtained as

$$k_{app} = \{k_{+1}[S] + k_{-1} + k_{+2} + k_{-2} + k_{+3} \pm \sqrt{(k_{+1}[S] + k_{-1} - k_{+2} - k_{-2} - k_{+3})^2 + 4k_{+2}(k_{-1} - k_{+3})}\}/2 \quad (8a)$$

By expanding the square root to a Taylor's series and taking the first two terms, $k_{app,fast}$ and $k_{app,slow}$ are expressed as

$$k_{app,fast} = k_{+1}[S] + k_{-1} + k_{+2}\frac{(k_{-1} - k_{+3})/k_{+1}}{(k_{-1} - k_{+3})/k_{+1} + \{[S] - [(k_{+2} + k_{-2})/k_{+1}]\}} \quad (9a)$$

$$k_{app,slow} = k_{+2}\frac{[S] - (k_{+2} + k_{-2})/k_{+1}}{(k_{-1} - k_{+3})/k_{+1} + \{[S] - [(k_{+2} + k_{-2})/k_{+1}]\}} + k_{-2} + k_{+3} \quad (10a)$$

From eq 3a and 4a, the following relationships are obtained:

$$[X_1]_{ss} = \frac{k_{-2} + k_{+3}}{k_{+2} + k_{-2} + k_{+3}}\frac{[S]}{K_m + [S]}[E]_{tot} \quad (11a)$$

$$[X_2]_{ss} = \frac{k_{+2}}{k_{+2} + k_{-2} + k_{+3}}\frac{[S]}{K_m + [S]}[E]_{tot} \quad (12a)$$

where

$$K_m = \frac{k_{-1}k_{-2} + k_{-1}k_{+3} + k_{+2}k_{+3}}{k_{+1}(k_{+2} + k_{-2} + k_{+3})} \quad (13a)$$

REFERENCES

Ando-Yamamoto, M., Hayashi, H., Sugiyama, T., Fukui, H., Watanabe, T., & Wada, H. (1987) *J. Biochem.* (Tokyo) *101*, 405–414.

Barboni, E., Voltattorni, C. B., D'Erme, M., Fiori, A., Minelli, A., & Rosei, M. A. (1982) *Life Sci. 31*, 1519–1524.

Dominici, P., Tancini, B., Barra, D., & Voltattorni, C. B. (1987) *Eur. J. Biochem. 169*, 209–213.

Johnson, G. F., Tu, J.-I., Shonka Bartlett, M. L., & Graves, D. J. (1970) *J. Biol. Chem. 245*, 5560–5568.

Kallen, R. G., Korpela, T., Martell, A. E., Matsushima, Y., Metzler, C. M., Metzler, D. E., Morozov, Yu. V., Ralston, I. M., Savin, F. A., Torchinsky, Yu. M., & Ueno, H. (1985) in *Transaminases* (Christen, P., & Metzler, D. E., Eds.) pp 37–108, John Wiley & Sons, New York.

Maras, B., Dominici, P., Barra, D., Bossa, F., & Voltattorni, C. B. (1991) *Eur. J. Biochem. 201*, 385–391.

Metzler, C. M., Metzler, D. E., & Jin, P. (1987) in *Biochemistry of Vitamin B_6* (Korpela, T., & Christen, P., Eds.) pp 111–113, Birkhäuser, Basel, Switzerland.

Minelli, A., Charteris, A. T., Borri Voltattorni, C., & John, R. (1979) *Biochem. J. 183*, 361–368.

Misono, H., & Soda, K. (1977) *J. Biochem.* (Tokyo) *82*, 535–543.

Nakazawa, H., Kumagai, H., & Yamada, H. (1974) *Biochem. Biophys. Res. Commun. 61*, 75–82.

O'Leary, M. (1971) *Biochim. Biophys. Acta 242*, 484–492.

Shaltiel, S., & Cortijo, M. (1970) *Biochem. Biophys. Res. Commun. 41*, 594–600.

Sprengart, M. L., Fatscher, H. P., & Fuchs, E. (1990) *Nucleic Acids Res. 18*, 1719–1723.

Tanaka, T., Horio, Y., Taketoshi, M., Imamura, I., Ando-Yamamoto, M., Kangawa, K., Matsuo, H., Kuroda, M., & Wada, H. (1989) *Proc. Natl. Acad. Sci. U.S.A. 86*, 8142–8146.

Vázquez, M. A., Muñoz, F., Donoso, J., & García Blanco, F. (1991) *Biochem. J. 279*, 759–767.

Voltattorni, C. B., Minelli, A., & Turano, C. (1971) *FEBS Lett. 17*, 231–235.

Voltattorni, C. B., Minelli, A., Vecchini, P., Fiori, A., & Turano, C. (1979) *Eur. J. Biochem. 93*, 181–188.

Yonaha, K., Misosno, H., Yamamoto, T., & Soda, (1975) *J. Biol. Chem. 250*, 6983–6989.